THE JOURNAL OF BIOLOGICAL CHEMISTRY
Vol. 273, No. 36, Issue of September 4, pp. 23150–23159, 1998
Printed in U.S.A.

Rate Constants for O_2 and CO Binding to the α and β Subunits within the R and T States of Human Hemoglobin*

(Received for publication, April 8, 1998, and in revised form, June 15, 1998)

Satoru Unzai‡, Raymund Eich§, Naoya Shibayama¶, John S. Olson§, and Hideki Morimoto‡

From the ‡Department of Biophysical Engineering, Faculty of Engineering Science, Osaka University, Toyonaka, Osaka 560, Japan, the §Department of Biochemistry and Cell Biology, Rice University, Houston, Texas 77251, and ¶Department of Physics, Jichi Medical School, Minamikawachi, Tochigi 329-04, Japan

Despite a large amount of work over the past 30 years, there is still no universal agreement on the differential reactivities of the individual α and β subunits in human hemoglobin. To address this question systematically, we prepared a series of hybrid hemoglobins in which heme was replaced by chromium(III), manganese(III), nickel(II), and magnesium(II) protoporphyrin IXs in either the α or β subunits to produce α_2(M)β_2(Fe)[1] and α_2(Fe)β_2(M) tetramers. None of the abnormal metal complexes react with dioxygen or carbon monoxide. The O_2 affinities of the resultant hemoglobins vary from 3 μM^{-1} (Cr(III)/Fe(II) hybrids) to 0.003 μM^{-1} (Mg(II)/Fe(II) hybrids), covering the full range expected for the various high (R) and low (T) affinity quaternary conformations, respectively, of human hemoglobin A_0. The α and β subunits in hemoglobin have similar O_2 affinities in both quaternary states, despite the fact that the R to T transition causes significantly different structural changes in the α and β heme pockets. This functional equivalence almost certainly evolved to maintain high n values for efficient O_2 transport.

In 1970, Perutz (1) published a detailed mechanistic interpretation of cooperative oxygen binding to hemoglobin (Hb). Two key structural features of the protein molecule were stressed. First, in deoxy-Hb, the ferrous iron atom was high spin and out of the plane of the porphyrin ring toward the proximal histidine (F8). In the low affinity or T state quaternary conformation, movement back into the plane of the heme was restricted. This restriction was postulated to be the major cause of reduced affinity in the T quaternary state (1). Over the past 30 years, various spectral and structural studies have shown that the R to T conformational transition causes ruffling and strain on the α heme group that results in large changes in its visible spectrum and can result in disruption of the αFe-His(F8) bond when NO is bound (2–5). Although tacitly accepted by most workers, there is less direct spectral or structural evidence for proximal strain in β subunits.

In the original paper, Perutz (1) also suggested that ligand binding to T state β subunits was sterically restricted by the presence of the His(E7) and Val(E11) side chains almost directly over the iron atom. As a result, Perutz (1) proposed that ligands first bind to α subunits. This binding then causes the switch from the low to the high affinity quaternary state in which the β subunits have a much more open β distal pocket and can readily bind oxygen. Perutz's proposal of an ordered addition of ligands conflicted with results from Gibson's group. Their experimental data suggested that significant kinetic and equilibrium differences between the Hb subunits occur only for ligands containing three or more non-hydrogen atoms and that the β and not α subunits are more sterically accessible to large ligands such as n-butyl isocyanide, even in the T state (6–10).

A myriad of experimental approaches were developed to resolve this controversy concerning functional differences between the subunits, including the following: (i) measurements of the ligand binding properties of the isolated α and β chains (3); (ii) discovery or development of spectral signals for ligation of the individual subunits within intact tetramers (11); (iii) selective chemical modification or mutation of key residues in the α and β chains (12, 13); (iv) separation of kinetic intermediates by cryogenic electrophoresis (14); (v) x-ray diffraction analysis of partially liganded Hb crystals (15); and (vi) construction of valency and metal hybrid Hbs in which one pair of subunits has an inert metal-porphyrin group and the other O_2- and CO-reactive heme groups (16–24). The latter approach is the most definitive with respect to assigning observed rate and equilibrium constants since only one type of subunit is capable of reacting with ligands.

Despite a large number of experiments and reports over the past 30 years, there is still no universal agreement on the differential reactivities of the individual subunits. Part of the problem is that the two-state model is an oversimplification. It is clear that multiple forms of the low affinity quaternary conformation occur, depending on pH and organic phosphate concentration (25, 26), and that there are alternative crystal forms of liganded Hb A_0 (27–29). In addition, Ackers and coworkers (30–32) have presented evidence for unique intermediate quaternary states, although some of the work with cyanomet hybrids is being challenged (33, 34). The other key problem is that the rate of interconversion of the R and T states is not always rapid with respect to oxygen and carbon monoxide binding. As a result, time courses for ligand binding to α(Fe)β(inert) and α(inert)β(Fe) hybrids are often biphasic, with rapid and slow phases representing very slowly interconverting R and T conformations, respectively.

The combination of conformational state polymorphism and relatively slow interconversion rates has made the interpretation of experiments with metal and valency hybrids much more complex than initially anticipated. Over 25 years ago, Cassoly and Gibson (17) showed that CO binding to the deoxy cyanomet hybrids, $\alpha_2(Fe^{3+}CN^-)\beta_2(Fe^{2+})$ and $\alpha_2(Fe^{2+})\beta_2(Fe^{3+}CN^-)$, is

* The costs of publication of this article were defrayed in part by the payment of page charges. This article must therefore be hereby marked "*advertisement*" in accordance with 18 U.S.C. Section 1734 solely to indicate this fact.

[1] The abbreviations used are: bis-Tris, 2,2-bis(hydroxymethyl)-2,2′,2″-nitrilotriethanol; IHP, inositol hexaphosphate; Cr(III)PPIX, chromium(III) protoporphyrin IX; Mn(III)PPIX, manganese(III) protoporphyrin IX; Ni(II)PPIX, nickel(II) protoporphyrin IX; Mg(II)PPIX, magnesium(II) protoporphyrin IX; M/Fe(II) hybrid Hb, metal-substituted hybrid hemoglobin in which hemes in either the α or β subunit are substituted with metalloprotoporphyrin IX; α_2(M)β_2(Fe), hybrid hemoglobin containing metalloprotoporphyrin IX in the α subunits and ferrous protoporphyrin IX in the β subunits; α_2(Fe)β_2(M), hybrid hemoglobin complementary to the preceding one.

heterogeneous. The fast and slow phases were assigned to CO binding to R and T state Hb, respectively, and the quaternary conformational transition between the fast and slow binding components was estimated to be extremely slow (less than 1 s^{-1}). Similar complex results were obtained for CO binding to the symmetrical Co(II)/Fe(II) and Mn(II)/Fe(II) hybrids (18–21). What was needed were metal substitutions that would lock the hybrid Hb tetramers into primarily R or T conformations, not mixtures. Such hybrids would allow unambiguous assignment of rate constants to the iron-containing subunit in one or the other of the quaternary states.

Over the past 12 years, Morimoto and co-workers (24, 35–39) have prepared and characterized metal-substituted hybrid Hbs using first transition metal ions. Some of the hybrid Hbs can be used as T or R state models. The definition of conformational state behavior is based historically and experimentally on O_2 binding properties. Low O_2 affinity comparable to that of the first oxygenation step of deoxy-Hb A_0 ($K_{O_2} \approx 0.003 - 0.01\ \mu M^{-1}$) refers to the T state, and high O_2 affinity comparable to that of the last oxygenation step of Hb A_0 ($K_{O_2} \approx 1 - 3\ \mu M^{-1}$) refers to the R state. In 1986 Shibayama *et al.* (35, 36) showed that, at neutral or low pH, Ni(II)/Fe(II) hybrids of human Hb show T state behavior with respect to oxygen binding and spectral properties. Luisi and Shibayama (37) and Luisi and co-workers (38) showed that these proteins crystallize in the deoxy form of Hb A_0 and have the structural features characteristic of the T quaternary state. The Ni(II) atom forms only 5- and 4-coordinate complexes which are characteristic of the deoxy T state. More recently, Park and co-workers (39)[2] prepared Mg(II)/Fe(II) hybrid Hbs that also show functional and structural characteristics of the low affinity T state. In this case, the Mg(II) atom forms only 5-coordinate complexes with porphyrin and globin, and as a result, Mg(II)/Fe(II) Hb crystallizes in the T quaternary conformation, even the presence of bound CO.

In contrast, Cr(III)/Fe(II) hybrids of human Hb show very high affinities for O_2 and the chemical and spectral characteristics of the R state (24). In this case, the Cr(III) atom has an ionic radius (0.62 Å) approximately equal to that of low spin Fe(II), forms strong hexacoordinate complexes with water or OH^- as an axial ligand, and is expected to fit in the flat plane of the porphyrin ring, and have a proximal His-Cr(III) bond as short as that in oxy-Hb (40–43). Similar arguments apply to Mn(III)-porphyrin complexes (21). However, the Cr(III)/Fe(II) hybrids are much more convenient to examine kinetically since this metal is inert to sodium dithionite.

In this work, we have used all four hybrids in an attempt to assign unambiguously rate and equilibrium constants for O_2 and CO binding to α and β subunits within T and R state-like conformations of Hb A_0. R state parameters were assigned based on measurements with Cr(III) and Mn(III) hybrids and T state parameters based on results for the Ni(II) and Mg(II) hybrids. The O_2 equilibrium properties of Cr(III)/Fe(II) and Ni(II)/Fe(II) hybrids have been studied previously. The K_2 values for O_2 binding to Fe(II) subunits in the Cr(III) hybrids are similar to the fourth equilibrium constant for O_2 binding to Hb A_0 (24). The K_1 values for O_2 binding to Fe(II) subunits in the Ni(II) hybrids are similar to the first O_2 binding equilibrium constant for Hb A_0 (35, 36, 44). Shibayama *et al.* (22) have also published rates for O_2 and CO binding to the Ni(II) hybrids in phosphate buffers. Morimoto and co-workers,[3] have shown that the Mn(III)/Fe(II) hybrids have O_2 affinities intermediate between those for the Cr(III) and Ni(II) hybrids, whereas the Mg(II)/Fe(II) hybrids have affinities for O_2 which are slightly lower than those of the Ni(II)-containing Hbs.[2] However, no kinetic studies with the Cr(III) and Mg(II) hybrids have been reported.

Our goal was to determine association and dissociation rate constants for O_2 and CO binding to all four types of metal hybrids under identical conditions. The results have provided two sets of kinetic parameters for α and β subunits thought to be in mostly T conformations, *i.e.* the Ni(II) and Mg(II) hybrids, and two sets of parameters for subunits in mostly R conformations, *i.e.* the Cr(III) and Mn(III) hybrids. These results have been compared with previous estimates of O_2 and CO ligand binding constants to provide a final resolution of the problem of differential reactivities of the α and β subunits. The absolute values of the kinetic parameters are very important for two other reasons. (i) They show that the addition of O_2 and CO to the α and β subunits is not ordered to any great extent, either at equilibrium or kinetically, and thus, the stereochemical mechanisms for cooperative ligand binding to each subunit need to be re-examined. (ii) These parameters also provide the starting points for evaluating the effects of mutagenesis on the ligand binding properties of recombinant Hbs and for designing more efficient Hb-based, O_2 delivery pharmaceuticals (45, 46).

EXPERIMENTAL PROCEDURES

Preparation of Metal-Fe(II) Hybrid Hemoglobins—Hb A_0 and its isolated chains were prepared in carbon monoxide forms as described by Fujii *et al.* (47). Cr(III)/Fe(II) hybrid Hbs were prepared as previously reported (24). Mn(III)/Fe(II) hybrid Hbs were prepared as described by Waterman and Yonetani (48). Ni(II)/Fe(II) hybrid Hbs were prepared as described by Shibayama *et al.* (35). Mg(II)/Fe(II) hybrid Hbs were prepared as described by Park *et al.* (39).

Measurements of CO Binding—CO binding to the deoxygenated metal/Fe(II) hybrid Hbs were measured using stopped-flow rapid mixing technique as described by Mathews *et al.* (49). Concentrated Hb samples were diluted in deoxygenated buffer to a concentration of 10 μM on a per metal basis. In order to ensure complete anaerobiosis, small amounts of sodium dithionite were added to solutions of Cr(III)/Fe(II) hybrids. Dithionite was not added to solutions of Ni(II)/Fe(II) and Mg(II)/Fe(II) hybrids. The oxygen affinities of the latter Hbs are so low that complete deoxygenation is easily attained without dithionite. The deoxygenated hybrid Hbs were mixed with anaerobic buffer containing 33.4 μM CO, and the resultant absorbance changes were measured at 436 nm. CO binding experiments were carried out at the following three pH conditions: 6.5, 7.4, and 8.4. When the hybrids showed monophasic time course, the data were fitted empirically to a single exponential expression as shown in Equation 1,

$$\Delta A_t = \Delta A_0 \exp(-k_{obs}t) \qquad \text{(Eq. 1)}$$

where ΔA_t is the observed absorbance change at time t; ΔA_0 is the total absorbance change; and k_{obs} was the observed pseudo first-order rate constant. In case of CO binding, $k_{obs} = k'_{CO}[CO]$, where k'_{CO} is the bimolecular CO association rate constant. When the hybrid Hbs showed biphasic time courses, the data were fitted to a two-exponential expression as shown in Equation 2,

$$\Delta A_t = \Delta A_0(F_f \exp(-k_f t) + (1 - F_f)\exp(-k_s t)) \qquad \text{(Eq. 2)}$$

where F_f is the fraction of fast reacting species, and k_f and k_s are the observed pseudo first-order rate constants for the fast and slow phases. For each phase, k'_{CO} was calculated by dividing of the observed rates, k_s and k_f, by [CO].

Measurements of CO Dissociation—CO dissociation rate constants were determined by mixing HbCO samples with buffer containing 1 atm of NO in the stopped-flow apparatus and monitoring displacement of bound carbon monoxide at 420 and 406 nm as described by Mathews *et al.* (50). The Hb samples were diluted to 10 μM on a per metal basis into anaerobic buffer containing 100 μM CO and then mixed with anaerobic buffer containing NO. Under these conditions, the observed replacement rate constant is equal to the CO dissociation constant, k_{CO} (50).

Measurements of O_2 Association—Oxygen rebinding to the metal-Fe(II) hybrids was measured after flash photolysis using the pulsed dye laser system described by Mathews *et al.* (50) and Rohlfs *et al.* (51). The Hb concentration was 200 μM on a per metal basis, and 1-mm path

[2] G. Miyazaki, K. M. Yun, T. Minagawa, M. Fujii, S. Y. Park, and H. Morimoto, manuscript in preparation.

[3] H. Morimoto, M. Masuda, and G. Miyazaki, unpublished work.

length cuvettes were used. Absorbance changes were measured at 436 nm. The observed pseudo first-order rate constant for bimolecular O_2 rebinding is given by Equation 3,

$$k_{obs} = k'_{O_2}[O_2] + k_{O_2} \quad \text{(Eq. 3)}$$

where k'_{O_2} is the O_2 association rate constant and k_{O_2} is the O_2 dissociation rate constant. Time courses were recorded at several different O_2 concentrations and values of k'_{O_2} and k_{O_2} were obtained from the slope and y intercept of plots of k_{obs} *versus* $[O_2]$. In the case of the Cr(III) and Mn(III) hybrids, the value of k_{O_2} is poorly defined in these plots since the absolute value is 10 to 100 times smaller than the observed rate constant at the lowest accessible $[O_2]$, usually air-equilibrated buffer. In the case of the Ni(II) and Mg(II) hybrids, the y intercept is defined, with dissociation rate constants on the order of 1000–2000 s^{-1}.

Measurements of O_2 Dissociation—O_2 dissociation rate constants were determined by mixing HbO_2 samples with buffer equilibrated with 1 atm CO in the stopped-flow apparatus, and the ligand replacement reaction was followed at 423 nm as described by Mathews *et al.* (50). The protein was diluted to 10 μM in buffers containing O_2 concentrations ranging from 262 μM (air) to 1250 μM (1 atm O_2). Under these conditions, the observed replacement rate, r_{obs}, is given by Equation 4.

$$r_{obs} = \frac{k_{O_2}}{\left(1 + \frac{k'_{O_2}[O_2]}{k'_{CO}[CO]}\right)} \quad \text{(Eq. 4)}$$

where k_{O_2} is the rate constant for O_2 dissociation from fully liganded (R state) Hb, and k'_{O_2} and k'_{CO} are the association rate constants for O_2 and CO binding to Hb_4X_3 intermediates, respectively (3, 13). Values of r_{obs} were measured as a function of $[CO]/[O_2]$, and the results were fitted to the hyperbolic expression in Equation 4 to obtain values of k_{O_2}. This approach could not be used to obtain k_{O_2} values for the Ni(II)/Fe(II) and Mg(II)/Fe(II) hybrids because the O_2 dissociation rate constants for these proteins are extremely large, ~2000 s^{-1}, and difficult to measure directly by rapid mixing.

All kinetic experiments were carried out in 50 mM Tris or bis-Tris,[1] 100 mM Cl^-, at 25 °C. Often three pH conditions were used as follows: 6.5, 7.4, and 8.4. When inositol hexaphosphate was added to the Hb solutions, the final [IHP] before mixing was 100 μM.

RESULTS

CO Association Constants—Rapid mixing time courses for the reaction of CO with α_2(Cr)β_2(Fe) and α_2(Fe)β_2(Cr) Hbs are biphasic (Fig. 1*A*). The CO association rate constants (k'_{CO}) and percentages of fast and slow components are listed in Table I. Under the same buffer conditions, the time courses for CO binding to the Ni(II)/Fe(II) and Mg(II)/Fe(II) hybrids are monophasic, even in the absence of organic phosphates (Fig. 1*B*). The values of k'_{CO} for these low affinity hybrids are also listed in Table I.

The fast CO-reacting phases for the high affinity Cr(III) hybrids are dominant at pH 7.4 and 8.4 in the absence of IHP. The k'_{CO} values for this phase are roughly independent of pH. In the absence of organic phosphates, k'_{CO} for the β(Fe) containing hybrid is slightly greater than that for the α(Fe) hybrid. Addition of IHP increases the fraction of the slow phase and decreases the values of k'_{CO} for both the fast and slow phases. However, the changes in the fast rate constants are very small compared with marked increases in the fraction of slow phase produced by decreasing pH and the presence of IHP.

The Cr(III)/Fe(II) hybrids bind oxygen almost non-cooperatively (n_{max} = 1.0–1.1) with very high affinities. The P_{50} values for these proteins at pH 7.4 and 8.4 in the absence of IHP are comparable to those of isolated α or β chains (24). Under these conditions, the deoxygenated Cr(III) hybrids appear to stay in an R state even in the absence of bound ligands. Consequently, we assigned the fast rate constants for the α_2(Fe)β_2(Cr) hybrid at pH 7.4 or 8.4 to that for CO binding to an α(Fe) subunit within an R state-like conformation of tetrameric Hb, and the fast rate constants for α_2(Cr)β_2(Fe) to those for CO binding to a β(Fe) subunit within this high affinity conformational state. These association rate constants, $k'_{\alpha CO}$ = 6 μM^{-1} s^{-1} and $k'_{\beta CO}$ = 7.4 μM^{-1} s^{-1}, are either equal or very close to those reported previously for R state forms of Hb A_0 (12, 21, 50). We used low heme concentrations in our experiments with the Cr(III) hybrids. As a result, an appreciable fraction of dimers was present. However, dimerization does not appear to affect the measured value of k'_{CO} for R state Hb because under most conditions the kinetic parameters for the last step in ligand binding to tetrameric Hb and those for binding to dimeric Hb are almost identical (12, 13, 52).

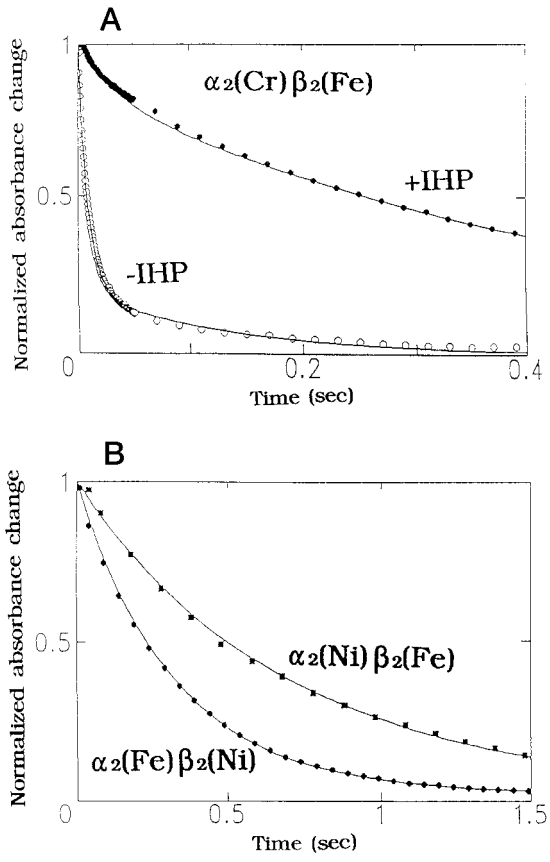

FIG. 1. **Normalized time courses for CO binding to Cr(III)/Fe(II) and Ni(II)/Fe(II) hybrid hemoglobins at pH 7.4, 25 °C.** Reactions were carried out in a stopped-flow, rapid mixing apparatus, and absorbance changes were measured at 436 nm. The concentrations after mixing were 5 μM Hb on a per metal basis and 16.7 μM CO. The *solid lines* represent fits to a single or two exponential expression. *A*, time courses for CO binding to α_2(Cr)β_2(Fe) in the absence and presence of 100 μM IHP. *B*, time courses for CO binding to α_2(Fe)β_2(Ni) and α_2(Ni)β_2(Fe) hybrids in the absence of IHP.

The time courses for CO binding to the Ni(II) and Mg(II) hybrids are very similar to each other and show much less dependence on pH and IHP. The association rate constants for CO binding to the α_2(Ni)β_2(Fe) and α_2(Mg)β_2(Fe) hybrids (k'_{CO} = 0.05 to 0.07 μM^{-1} s^{-1}) are consistently 2-fold smaller than those for the corresponding α(Fe) containing hybrid Hbs (k'_{CO} = 0.12 to 0.16 μM^{-1} s^{-1}; Table I, part B, pH 6.5, 7.4 ± IHP). Our values for the Ni(II) and Mg(II) hybrids agree well with those reported previously for T state forms of cyanomet valency and other metal hybrid Hbs. In the presence of IHP, α(Fe) subunits in cyano-Fe(III)/Fe(II), Co(II)/Fe(II), and Mn(II)/Fe(II) hybrids show larger association rate constants for CO binding than those for β(Fe) subunits (17–20). Shibayama *et al.* (22) obtained a rate constant of 0.15 μM^{-1} s^{-1} for bimolecular CO rebinding to both the α(Fe) and β(Fe) containing Ni(II) hybrids after flash photolysis in 0. 1 M phosphate at pH 6.6. Their higher value for the β(Fe) k'_{CO} may be due to incomplete conversion of the hybrid to the T state during the time between

TABLE I
Association rate constant for CO binding k'_{CO} to metal hybrids of human deoxyhemoglobin at 25 °C

Conditions were 50 mM Tris or bis-Tris, 100 mM NaCl. Protein concentration was 5 μM on a per metal basis after mixing. CO concentration was 16.7 μM after mixing. Reactions were followed at 436 nm. The reactions of the deoxy Fe(II)/Cr(III) were always biphasic, and the percentages of the fast and slow components are shown. The reactions with HbA_0 and the Fe(II)/Ni(II) and Fe(II)/Mg(II) were monophasic, and only a single rate constants was determined. +IHP indicates that 100 μM inositol hexaphosphate was added to the protein solution prior to mixing with CO.

pH	IHP	HbA_0	$\alpha_2(Fe)\beta_2(Cr)$		$\alpha_2(Cr)\beta_2(Fe)$	
			Fast[a]	Slow[b]	Fast	Slow
			$\mu M^{-1}\ s^{-1}$			
A. k'_{CO} for deoxy HbA_0 and Fe(II)/Cr(III) hybrids						
6.5	−	0.18	3.2 (39%)[c]	0.28 (61%)[d]	6.1 (79%)	0.28 (21%)
	+	0.095	6.6 (6%)	0.15 (94%)	2.3 (22%)	0.11 (78%)
7.4	−	0.23	5.0 (86%)	0.49 (14%)	7.0 (86%)	0.47 (14%)
	+	0.081	4.8 (38%)	0.16 (62%)	2.1 (20%)	0.13 (80%)
8.4	−	0.32	7.0 (90%)	1.3 (10%)	7.7 (90%)	0.57 (10%)
	+	0.14	5.9 (73%)	0.44 (27%)	6.5 (83%)	0.26 (17%)

pH	IHP	$\alpha_2(Fe)\beta_2(Ni)$	$\alpha_2(Ni)\beta_2(Fe)$	$\alpha_2(Fe)\beta_2(Mg)$	$\alpha_2(Mg)\beta_2(Fe)$
		$\mu M^{-1}\ s^{-1}$			
B. k'_{CO} for deoxy Fe(II)/Ni(II) and Fe(II)/Mg(II) hybrids					
6.5	−	0.15	0.085	0.12	0.051
	+	0.11	0.065	0.12	0.047
7.4	−	0.19	0.086	0.19	0.041
	+	0.12	0.061	0.14	0.037
8.4	−	0.34	0.095	0.20	0.058
	+	0.21	0.068	0.13	0.047

[a] The bimolecular CO association rate constant for the fast phases.
[b] The bimolecular CO association rate constant for the slow phases.
[c] The fraction of fast phases.
[d] The fraction of slow phases.

TABLE II
Rate constants for CO dissociation, k_{CO}, from metal hybrids of human hemoglobin at 25 °C

Conditions were as follows: 50 mM Tris or bis-Tris, 100 mM NaCl at 25 °C. Protein concentration was 5 μM on a metal basis after mixing. CO and NO concentrations were 50 and 1000 μM after mixing, respectively. The replacement of bound CO by NO was followed at 420 or 406 nm. All of the reactions were monophasic. +IHP indicates that 100 μM inositol hexaphosphate was added to the protein solution prior to mixing. The abbreviation ND means not determined.

pH	IHP	HbA_0	$\alpha_2(Fe)\beta_2(Cr)$	$\alpha_2(Cr)\beta_2(Fe)$	$\alpha_2(Fe)\beta_2(Mn)$	$\alpha_2(Mn)\beta_2(Fe)$
			s^{-1}			
A. k_{CO} for the liganded forms of HbA_0 and Fe(II)/Cr(III) and Fe(II)/Mn(III) hybrids						
6.5	−	0.011	0.014	0.0087	0.018	0.0097
	+	0.012	0.013	0.0095	0.018	0.012
7.4	−	0.0090	0.013	0.0071	0.012	0.0069
	+	0.0096	ND	ND	ND	ND
8.4	−	0.012	0.011	0.0071	0.010	0.0077

pH	IHP	$\alpha_2(Fe)\beta_2(Ni)$	$\alpha_2(Ni)\beta_2(Fe)$	$\alpha_2(Fe)\beta_2(Mg)$	$\alpha_2(Mg)\beta_2(Fe)$
		s^{-1}			
B. k_{CO} for the liganded forms of Fe(II)/Ni(II) and Fe(II)/Mg(II) hybrids					
6.5	−	0.027	0.032	0.10	0.024
	+	0.18	0.21	0.23	0.17
7.4	−	0.020	0.020	0.028	0.017
	+	0.022	0.047	0.051	0.024
8.4	−	0.014	0.010	0.016	0.013
	+	0.014	0.010	0.016	0.012

photolysis and ligand rebinding or to the effects of inorganic phosphate.

Our T state k'_{CO} values for β(Fe) subunits based on results for Ni(II) and Mg(II) hybrids are ~2-fold smaller than those based on studies with mutant and native human Hbs. Mathews *et al.* (49) reported that $k'_{CO} = 0.12 \pm 0.03$ and 0.18 ± 0.05 $\mu M^{-1}\ s^{-1}$ for T state α(Fe) and β(Fe) subunits, respectively. These assignments were based on comparisons between Hbs containing one mutated and one native subunit. Perrella *et al.* (14) reported similar values, $k'_{\alpha CO} = 0.10 \pm 0.04$ $\mu M^{-1}\ s^{-1}$ and $k'_{\beta CO} = 0.15 \pm 0.02$ $\mu M^{-1}\ s^{-1}$, based on detailed analysis of the overall CO-binding reaction. In their work, cryogenic isoelectric focusing was used to separate the partially liganded tetrameric intermediates. Both sets of authors concluded that the α(Fe) and β(Fe) subunits have equivalent rates of CO binding within the T state since the errors in their individual subunit rate constants were greater than or equal to the differences between them.

CO Dissociation Constants—The time courses for NO replacement of bound CO were monophasic for all of the hybrid Hbs examined, regardless of pH and the presence of IHP. CO dissociation rate constants (k_{CO}) for the Cr(III), Mn(III), Ni(II), and Mg(II) hybrids and native Hb A_0 are listed in Table II. The k_{CO} values for the Mn(III) and Cr(III) hybrids are similar to that for fully liganded Hb A_0, depend little on reaction conditions, and can be used to assign rate constants for CO dissociation from α(Fe) and β(Fe) subunits within R quaternary states: $k_{\alpha CO} = 0.012 \pm 0.001$ and $k_{\beta CO} = 0.007 \pm 0.001$ s^{-1} (Table V).

In contrast, the k_{CO} values for the Ni(II) and Mg(II) hybrids are affected greatly by pH and the addition of inositol hexaphosphate. The presence of two bound CO molecules shifts these hybrids from T toward R quaternary conformations in the absence of organic phosphates, even at pH 6.5. Shibayama *et al.* (35) have shown that inositol hexaphosphate can shift the CO-liganded Ni(II)/Fe(II) hybrid to the T state at pH 6.5. As shown in Table II, part B, addition of IHP causes dramatic 10–20-fold increases in the CO dissociation rate constants for both the Ni(II) and Mg(II) hybrids. The k_{CO} values for the α(Fe) and β(Fe) subunit within these hybrids have been assigned as the rate constants for CO dissociation from T state Hb, *i.e.* $k_{\alpha CO} = 0.21\ s^{-1}$ and $k_{\beta CO} = 0.19\ s^{-1}$ (Table VI). Sharma *et al.* (53, 54) and Simolo *et al.* (55) showed that the rate constant for CO dissociation from native $Hb_4(CO)$ is in the range 0.1 to 0.2 s^{-1}. Samaja *et al.* (56) reported similar rate constants for the dissociation of CO from mono-liganded Hb A_0 and assigned tentative values for the individual subunits, 0.16–0.22 s^{-1} for α(Fe) subunits and 0.10–0.15 s^{-1} for β(Fe) subunits.

Photochemical Spectral Changes Associated with Cr(III) and Mg(II) Protoporphyrins—Flash photolysis time courses for the bimolecular O_2 rebinding to all four metal hybrid Hbs were recorded at several different ligand concentrations. In addition to the absorbance changes associated with Fe-ligand bond formation, an "extra" rapid phase was observed for the Cr(III) and Mg(II) hybrids (*i.e.* Fig. 2 *inset* and Fig. 6). Since both these hybrids are photosensitive, the extra fast phases probably originate from excited states of the Cr(III) and Mg(II) porphyrins. In the case of the Mg(II) hybrids, the extra absorbance transition appears in the initial microsecond region and overlaps with the fast or R state phase for bimolecular O_2 rebinding. The wavelength dependence of this absorbance change is very similar to the difference spectrum between the triplet state and the ground state of Mg(II)PPIX (57). Both difference spectra show an isosbestic point at 432 ± 1 nm and a broad peak around 475 nm. This correspondence suggests strongly that the extra fast phase for the Mg(II) hybrids is due to decay of the photoexcited triplet state of Mg(II)PPIX and not ligand binding. In the case of the Cr(III) hybrid, there is an initial absorbance change that decays in ~2.5 μs, shows no dependence on $[O_2]$, and is too rapid to interfere with measurements of ligand rebinding. Shibayama *et al.* (22) observed similar spectral changes associated with Ni(II)PPIX during and after photolysis of deoxygenated Ni(II)/Fe(II) hybrids in the 100-ps time region. In the

latter case, the photoexcited state decays much too rapidly to be observed in microsecond photolysis experiments.

Rates of O_2 Binding to Cr(III) and Mn(III) Hybrids—Time courses for O_2 rebinding to the Cr(III)- and Mn(III)-Fe(II) hybrids are monophasic and representative of high affinity R states at neutral and high pH in the absence of IHP (Figs. 2 and 3). The observed first order rates show a linear dependence on $[O_2]$ (Fig. 4). The *y* intercepts in these plots are close to zero with respect to the experimental values on the *y* axis, which range from ~10,000 to 100,000 s^{-1}. Under these conditions, k'_{O_2} for the β(Fe) subunits is roughly 2-fold greater than that for the α(Fe) subunits: $k'_{\beta O_2} \approx 80\ \mu M^{-1}\ s^{-1}$ *versus* $k'_{\alpha O_2} \approx 40\ \mu M^{-1}\ s^{-1}$, for both the Cr(III) and Mn(III) hybrids (Table III, part A). These values are in good agreement with previous measurements of R state O_2 association rate constants based on mutant and chemically modified Hbs (12, 13, 50, 52, 58).

Addition of IHP and lowering the pH cause complex changes in the time course for O_2 rebinding to the Cr(III) and Mn(III) hybrids (Fig. 3 and Table III, part A). Both conditions promote formation of low affinity conformations. As result, slow ligand association phases are observed and become dominant at pH 6.5 in presence of inositol hexaphosphate. The observed rate constants for these slow phases are similar to those observed for O_2 binding to Ni(II) and Mg(II) hybrids in the absence of organic phosphates (see Ref. 22; Table III, part B).

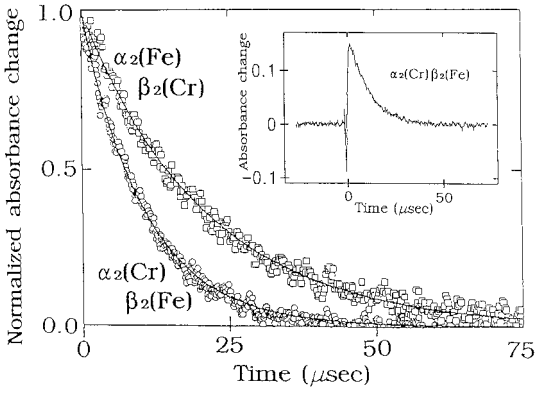

FIG. 2. **Normalized time courses for the recombination of Cr(III)/Fe(II) hybrid hemoglobins with 1260 μM O_2 at pH 7.4 in the absence of IHP.** The *solid lines through the symbols* represent fits to a single exponential expression. The *inset* shows observed absorbance changes for the recombination of α_2(Cr)β_2(Fe) with 1260 μM O_2, including the very rapid spectral change associated with photoexcited Cr(III)PPIX.

Rate constants for O_2 dissociation from the high affinity forms of Cr(III) and Mn(III) hybrids were obtained by analyzing time courses for the displacement of bound oxygen by carbon monoxide using Equation 4. The resultant values of k_{O_2} are given in Table IV, part A. At pH 7.4 and 8.4, these hybrids remain completely in the high affinity quaternary conformation, and the rate parameters can be assigned unambiguously to the R state. There is good agreement between the Cr(III) and Mn(III) hybrids, with $k_{\alpha O_2} \approx 16\ s^{-1}$ and $k_{\beta O_2} \approx 32\ s^{-1}$ for both types of proteins. These values are consistent with the low values of the *y* intercept in plots of k_{obs} *versus* $[O_2]$ obtained from the flash photolysis experiments (Fig. 4). They also agree with previously reported values of k_{O_2} for the R state subunits (7, 12, 13, 50, 52, 58)

Rates of O_2 Binding to Ni(II) and Mg(II) Hybrids—At pH 7.4, the time courses for O_2 rebinding to Ni(II)-Fe(II) hybrids are biphasic in the absence of IHP and become monophasic upon addition of IHP (Fig. 5). Plots of the observed first-order rate constants *versus* $[O_2]$ are linear, and the slopes are reported as k'_{O_2} values in Table III, part B. Similar behavior was observed for the two Mg(II) hybrids, but in this case the fast phase for O_2 rebinding to the Fe(II) subunits is obscured by the spectral changes associated with photoexcited Mg(II)PPIX (Fig. 6). Plots of k_{obs} for the slow phases of this protein *versus* $[O_2]$ are also linear (Fig. 7), and the bimolecular rate constants in the absence and presence of IHP at pH 7.4 are given in Table III, part B.

With one exception, the fraction of slow O_2 rebinding does not show much dependence on ligand concentration for the Ni(II) and Mg(II) hybrids. In the case of $\alpha_2(FeO_2)\beta_2$(Mg) the magnitude of the slow phase decreased significantly as $[O_2]$ was increased in the absence of IHP at pH 7.4. This result suggests that a significant fraction of the initial $\alpha_2(FeO_2)\beta_2$(Mg) complex is in a high affinity, R state-like conformation and that the rate of the R to T transition after photolysis is on the same order as that due to ligand recombi-

TABLE III

Bimolecular association rate constants, k'_{O2}, for O_2 rebinding to the oxygenated forms of metal hybrid of human hemoglobin after laser photolysis at 25 °C

Conditions were as follows: 50 mM Tris or bis-Tris, 100 mM NaCl. Protein concentration was 200 μM on a metal basis. Three O_2 concentrations were used for the Fe(II)/Cr(III) and Fe(II)/Mn(III) hybrids: 262, 630, or 1260 μM, and the slope of k_{obs} *versus* $[O_2]$ for the fast and slow phases are given below as k'_{O2} values (Fig. 4). For the Ni(II)/Fe(II) and Mg(II)/Fe(II) hybrid HbO_2 values, four O_2 concentrations were used: 63, 262, 630, or 1260 μM, and again the slope of k_{obs} *versus* $[O_2]$ is listed below. The *y* axis intercept of these plots are given as the k_{O2} values in Table IV (Fig. 7). One mm pathlength cells were used, and the time courses were followed at 436 nm. +IHP indicates that 100 μM inositol hexaphosphate was added to the protein solution. When two phases were observed, two rates are reported, and the percentage of the fast and slow absorbance changes are shown in parentheses (see Figs. 3–5).

pH	IHP	α_2(Fe)β_2(Cr)		α_2(Cr)β_2(Fe)		α_2(Fe)β_2(Mn)		α_2(Mn)β_2(Fe)	
		Fast	Slow	Fast	Slow	Fast	Slow	Fast	Slow
		$\mu M^{-1}\ s^{-1}$		$\mu M^{-1}\ s^{-1}$		$\mu M^{-1}\ s^{-1}$		$\mu M^{-1}\ s^{-1}$	
A. k'_{O2} for Fe(II)/Cr(III) and Fe(II)/Mn(III) hybrid hemoglobins									
6.5	−	31		64		36		69 (70%)	4.3 (30%)
	+		12	58 (60%)	6.2 (40%)		10		2.4
7.4	−	38		78		36		85 (90%)	9.1 (10%)
	+	49 (70%)	10 (30%)	67		35 (70%)	8.2 (30%)	73 (50%)	2.9 (50%)
8.4	−	40		80		36		77	
	+	40		80		36		76	
pH	IHP	α_2(Fe)β_2(Ni)		α_2(Ni)β_2(Fe)		α_2(Fe)β_2(Mg)		α_2(Mg)β_2(Fe)	
		Fast	Slow	Fast	Slow	Fast	Slow	Fast	Slow
		$\mu M^{-1}\ s^{-1}$		$\mu M^{-1}\ s^{-1}$		$\mu M^{-1}\ s^{-1}$		$\mu M^{-1}\ s^{-1}$	
B. k'_{O2} for Fe(II)/Ni(II) and Fe(II)/Mg(II) hybrid hemoglobins									
7.4	−	45 (70%)	5.9 (30%)	45 (40%)	7.2 (60%)	ND	5.3	ND	6.1
	+		11		5.8	ND	11	ND	4.0

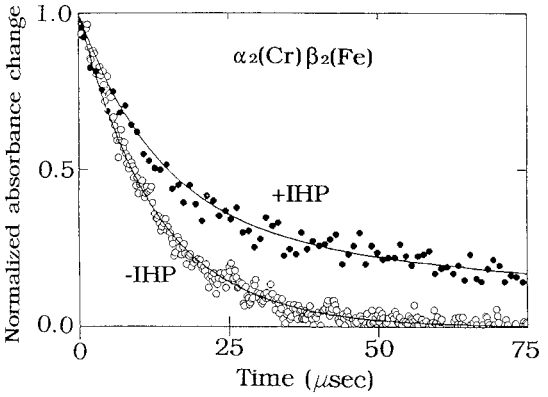

FIG. 3. **Normalized time courses for the recombination of α_2(Cr)β_2(Fe) with 1260 μM O_2 at pH 6.5 in the absence (*open circles*) and presence of 100 μM IHP (*closed circles*).** The *solid lines* represent fits to one and two exponential expressions.

TABLE IV

Rate constants for O_2 dissociation, k_{O2}, from metal hybrids of human hemoglobin at 25 °C

Conditions were as follows: 50 mM Tris or bis-Tris, 100 mM NaCl. Values of k_{O2} for the Fe(II)/Cr(III) and Fe(II)/Mn(III) hybrids were determined by measuring the observed rate for the displacement of bound O_2 by CO as a function of the ratio [CO]/[O_2] reactions. Protein concentration was 5 μM on a metal basis after mixing. Three [O_2] were used: 131, 315, or 630 μM after mixing, and [CO] was fixed at 500 μM after mixing. O_2–CO replacement reaction was followed at 423 nm. Values of k_{O2} for the low affinity Fe(II)/Ni(II) and Fe(II)/Mg(II) hybrids were estimated from the *y* intercept of plots of the observed rate of O_2 rebinding *versus* [O_2] based on the laser photolysis experiments described in Fig. 7. In this case, the protein concentration was 200 μM on a per metal basis, and the O_2 concentrations used were 63, 252, 630, and 1260 μM. O_2 rebinding was followed at 436 nm. +IHP indicates that 100 μM inositol hexaphosphate was added to the protein solution.

pH	IHP	α_2(Fe)β_2(Cr)	α_2(Cr)β_2(Fe)	α_2(Fe)β_2(Mn)	α_2(Mn)β_2(Fe)
			s^{-1}		
A. k_{O2} for the liganded forms of Fe(II)/Cr(III) and Fe(II)/Mn(III) hybrid hemoglobins					
6.5	–	28	47	21	26
7.4	–	17	31	16	29
8.4	–	14	31	12	25
pH	IHP	α_2(Fe)β_2(Ni)	α_2(Ni)β_2(Fe)	α_2(Fe)β_2(Mg)	α_2(Mg)β_2(Fe)
			s^{-1}		
B. k_{O2} for Fe(II)/Ni(II) and Fe(II)/Mg(II) hybrid hemoglobins					
7.4	–	200	500	600	800
	+	4300	1300	5200	2100

nation. The value of n_{max} is 1.2 for oxygen binding to α_2(Fe)β_2(Mg) at pH 7.4, indicating that some R state character is generated by ligand binding.[2] Despite this complexity, the observed rate constants for the slow phase of O_2 rebinding to the Mg(II) hybrids exhibit a simple dependence on ligand concentration which is consistent with that observed for the low affinity Ni(II) hybrids (Fig. 7; Table III, part B).

Since all available structural and functional data suggest that the Ni(II) and Mg(II) hybrids form predominantly low affinity conformations, the rate constants for the slow phases of O_2 rebinding to these proteins have been assigned to the subunits with T quaternary conformations. The observed values at pH 7.4 in the absence of IHP, $k'_{\alpha O_2}$ = 5.6 μM^{-1} s^{-1} and $k'_{\beta O_2}$ = 6.7 μM^{-1} s^{-1}, are very similar to those reported previously for T state subunits in native Hb A_0 and Ni(II) hybrids (5–10 μM^{-1} s^{-1}; Refs. 22 and 59).

Rate constants for O_2 dissociation from the Ni(II) and Mg(II) hybrids were estimated from the *y* intercepts of plots of k_{obs} for the slow phases observed after flash photolysis (see Fig. 7). The resultant values are listed in Table IV, part B. In the absence

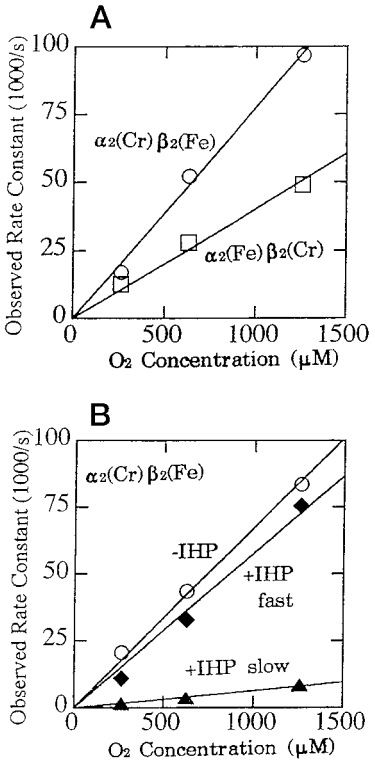

FIG. 4. **Dependence of the observed rates of rebinding to Cr(III)/Fe(II) hybrid hemoglobins on O_2 concentration.** The ordinate gives the fitted first-order rate in units of 1000 s^{-1} and, the *abscissa* is initial free [O_2] in μM. The *solid lines* represents fits to Equation 3. *A*, α_2(Fe)β_2(Cr) (*open squares*); α_2(Cr)β_2(Fe) (*open circles*). Conditions: 50 mM bis-Tris, 100 mM Cl^-, pH 7.4, 25 °C, in the absence of IHP. *B,* observed rate constants for α_2(Cr)β_2(Fe) in the absence of IHP (*open circles*) and for the fast (*closed diamonds*) and slow (*closed triangles*) phases in the presence of 100 μM IHP. Conditions: 50 mM bis-Tris, 100 mM Cl^-, pH 6.5, 25 °C

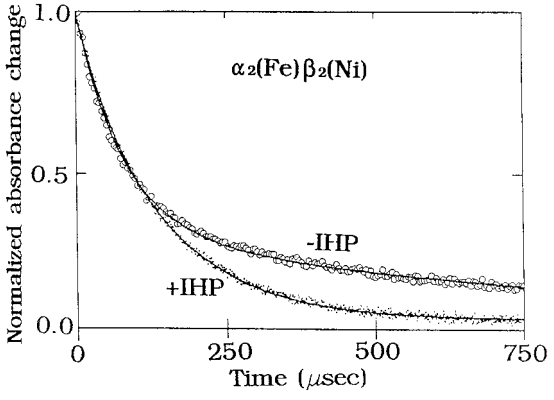

FIG. 5. **Normalized time courses for the recombination of α_2(Fe)β_2(Ni) with 262 μM O_2 in the absence and presence of 100 μM IHP at pH 7.4.** Absorbance changes were observed at 436 nm after photolysis with a 300-ns laser pulse. The *solid lines* represent fits to one and two exponential expressions.

of IHP, k_{O_2} is estimated to be roughly 400 s^{-1} for α(Fe) subunits and 650 s^{-1} for β(Fe) subunits. Addition of IHP increases the dissociation rate constant for both subunits, but the largest effect is on k_{O_2} for α(Fe) subunits, which increases to a value approaching 5,000 s^{-1} (Fig. 7*B*; Table IV, part B). IHP also selectively increases the association rate constants for O_2 binding to T state α(Fe) subunits as shown in Fig. 7 and Table IV, part B. When IHP is added to α_2(Fe)β_2(Ni), O_2 rebinding becomes monophasic and shows an observed rate that is significantly greater than that observed for the slow phase in the absence of the organic phosphate. This marked increase is

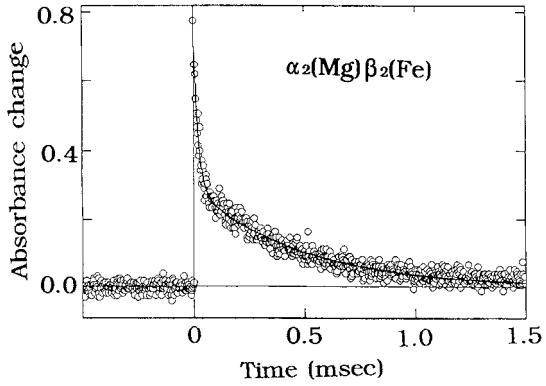

FIG. 6. **Time course for the recombination of α_2(Mg)β_2(Fe) with 262 μM O_2 at pH 7.4 in the absence of IHP.** Absorbance changes were observed at 436 nm after photolysis with a 300-ns laser pulse. The *solid line* represents a fit to a two-exponential expression.

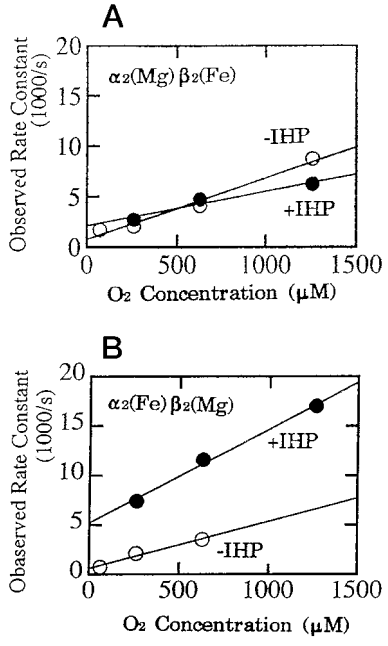

FIG. 7. **Dependence of the observed rates of slow rebinding to Mg(II)/Fe(II) hybrid hemoglobins on O_2 concentration.** Conditions: 50 mM bis-Tris, 100 mM Cl^-, pH 7.4, 25 °C. The *ordinate* gives the fitted first-order rate in units of 1000 s^{-1}, and the *abscissa* is initial free [O_2] in μM. The *solid lines* represents fits to Equation 3. *A*, observed rate constants for α_2(Mg)β_2(Fe) in the absence (*open circles*) and presence (*closed circles*) of IHP. *B*, observed rate constants for α_2(Fe)β_2(Mg) in the absence (*open circles*) and presence (*closed circles*) of IHP.

observed to be due to ~2 and ~10-fold increases in k'_{O_2} and k_{O_2}, respectively (see Equation 3).

DISCUSSION

Rate and Equilibrium Constants for Ligand Binding to R State Hemoglobin Subunits—Summaries of our new and previous assignments of rate and equilibrium constants for CO and O_2 binding to the individual α(Fe) and β(Fe) subunits within R or T state-like Hb conformations are given in Tables V–VIII. When corrected for differences in temperatures, the largest discrepancies for a given subunit and quaternary structure are ≤2-fold. The assignment of rate constants to the individual α(Fe) and β(Fe) subunits is unambiguous in the case of the Cr(III), Mn(III), Ni(II), and Mg(II) hybrid Hbs since the partner subunit is incapable of binding ligands. The assignments for mutant and chemically modified Hbs are based on the assumption that only the rate constants of the modified subunit are affected and often require detailed analyses and comparisons between several modified proteins to obtain rate constants for the native subunits (13). In our view, the agreement among the values reported in Tables V–VIII is remarkably good.

We have used the Cr(III) and Mn(III) hybrids at pH 7.4 and 8.4 in the absence of phosphates as models for R state Hb. The assignment of rate parameters to these proteins is straightforward since at neutral or high pH in the absence of IHP the time courses are predominantly one phase (Figs. 1*A*, 2, and 3; Tables I, part *A,* to IV, part A). The α(Fe) and β(Fe) subunits in R state Hb bind CO with roughly equal association rate constants, $k'_{\alpha CO} \approx k'_{\beta CO} \approx 7\ \mu M^{-1}\ s^{-1}$, and only slightly different dissociation rate constants, $k_{\alpha CO} = 0.012$ *versus* $k_{\beta CO} = 0.007\ s^{-1}$. In the case of O_2 binding, the β(Fe) subunits exhibit 2-fold higher association and dissociation rate constants than those for the α(Fe) subunits as follows: $k'_{\beta O_2} = 76\ \mu M^{-1}\ s^{-1}$ *versus* $k'_{\alpha O_2} = 36\ \mu M^{-1}\ s^{-1}$ and $k_{\beta O_2} = 32\ s^{-1}$ *versus* $k_{\alpha O_2} = 16\ s^{-1}$. However, the association equilibrium constants for O_2 binding to R state α(Fe) and β(Fe) subunits are identical: $K_{\alpha O_2} \approx K_{\beta O_2} \approx 2.4\ \mu M^{-1}$ at 25 °C in the absence of phosphates.

Rate Parameters for T State Hemoglobin Subunits—The Ni(II) and Mg(II) hybrids serve as models for T state Hb at pH 7.4 in the presence and absence of IHP. Assignment of association rate constants for CO binding is straightforward and unambiguous in stopped-flow experiments. When the deoxygenated forms of the Ni(II) and Mg(II) hybrids are mixed with CO, simple monophasic time courses are observed and can be assigned to reactions with T state subunits (Fig. 1*B*). These data show that T state α(Fe) subunits react about 2 times more rapidly with carbon monoxide than T state β(Fe) subunits, $k'_{\alpha CO} = 0.16\ \mu M^{-1}\ s^{-1}$ *versus* $k'_{\beta CO} = 0.07\ \mu M^{-1}\ s^{-1}$, and that this difference persists in the presence of IHP. These values do differ significantly from previous ones derived from studies with mutant and native Hbs. Experiments with the latter proteins suggested either equal rate constants for CO binding or slightly greater values for T state β(Fe) subunits (13, 14, 49). In our view, the assignments based on the metal hybrids are the least ambiguous since the differences between the ferrous subunits can be seen directly in the observed time courses (Fig. 1*B*).

In contrast, it proved difficult to assign rate constants for CO dissociation from T state subunits. The observed rate constant is a weighted sum of the R and T rates since these conformations interconvert more rapidly that CO dissociation. In the absence of IHP, only the α_2(Fe)β_2(Mg) hybrid at pH 6.5 showed a dissociation constant, ~0.1 s^{-1}, high enough to be due to a predominance of T state protein (Table II, part B). However, in the presence of IHP at pH 6.5, the observed rates for all four Ni(II) and Mg(II) hybrids do appear to be due exclusively to T state conformations. Under these conditions, the α(Fe) and β(Fe) subunits show roughly equal rates of CO dissociation, ~0.2 s^{-1} (Table VI).

The assignment of T state O_2 binding parameters was made easier by previous analyses of oxygen equilibrium curves for both the Ni(II) and Mg(II) hybrids (35, 36).[2] Association rate constants for the T state subunits were taken from analyses of the concentration dependence of the slow phases recorded after laser photolysis of the oxygenated forms of the Ni(II) and Mg(II) hybrids. Then the K_1 values reported for equilibrium O_2 binding to these hybrids were used to compute dissociation rate constants for the T state, Fe(II) subunits, *i.e.* $k_{O_2} = k'_{O_2}/K_1$. The average of the k_{O_2} values obtained for the Ni(II) and Mg(II) hybrids are reported in Table VIII. The numbers in parentheses are the *y* intercepts from the plots of k_{obs}(slow) *versus* [O_2] from the photolysis experiments (see Fig. 7). In our view, combining the equilibrium and kinetic measurements provides a

TABLE V

Rate and equilibrium constants for CO binding to the R or T states of human hemoglobin A_0, CO binding to the R quaternary state

The k'_{RCO} values for this work were computed as the average of fast association rate constants for CO binding to the Fe(II)/Cr(III) hybrids at pH 7.4 and 8.4 in the absence of IHP (Table 1, part A). The k_{RCO} values were computed from the average of those observed for the Fe(II)/Cr(III) and Fe(II)/Mn(III) hybrids at pH 7.4 and pH 8.4 ± IHP (Table II, part A). The equilibrium constants for CO binding to the subunits within R state hemoglobin were calculated from the ratio of the rate constants, $K_{RCO} = k'_{RCO}/k_{RCO}$. The parameters based on the metal hybrids are compared with those obtained from analyzing mutant hybrids (50) and native human hemoglobin using *p*-hydroxybenzoate modification of βCys-93 to enhance the differences between the subunits (12).

Subunit	Hemoglobin (Ref.)	Condition	k'_{RCO}	k_{RCO}	K_{RCO}
			$\mu M^{-1}\ s^{-1}$	s^{-1}	μM^{-1}
α(Fe)	Cr(III), Mn(III) hybrids (this work)	pH 7.4, 8.4, 25 °C	6.0	0.012 ± 0.001	510
	Mutant hybrids (50)	pH 7.0, 20 °C	2.9 ± 0.5	0.005 ± 0.002	600 ± 260
	Native HbA_0 (12)	pH 7.4, 25 °C	5 ± 1	0.008 ± 0.002	600 ± 190
β(Fe)	Cr(III), Mn(III) hybrids (this work)	pH 7.4, 8.4, 25 °C	7.4	0.007 ± 0.001	1,000
	Mutant hybrids (50)	pH 7.0, 20 °C	7.1 ± 2.4	0.007 ± 0.003	1,000 ± 550
	Native HbA_0 (12)	pH 7.4, 25 °C	15 ± 3	0.011 ± 0.002	1,400 ± 380

TABLE VI

Rate and equilibrium constants for CO binding to the R and T states of human hemoglobin A_0, CO binding to the T quaternary state

The k'_{TCO} values for this work were computed as the average of slow association rate constants for CO binding to the Fe(II)/Ni(II) hybrids at pH 6.5 and 7.4 in the absence and presence of 100 μM of IHP (Table I, part B). The k_{TCO} values were computed from the average of those observed for the same hybrids at pH 6.5 in the presence of 100 μM of IHP (this is the only condition in which the di-liganded hybrids showed T state behavior, see Table II, part B). The equilibrium constants for CO binding to the subunits within T state hemoglobin were calculated from the ratio of the rate constants. The k'_{TCO} values based on the metal hybrids are compared to those obtained from analyzing Mn(II)/Fe(II) hybrids (20), recombinant mutant hybrids (50) and native human hemoglobin using cryoscopic isoelectric focusing techniques to resolve the various intermediates (14). ND, not determined.

Subunit	Hemoglobin (Ref.)	Condition	IHP	k'_{TCO}	k_{TCO}	K_{TCO}
				$\mu M^{-1}\ s^{-1}$	s^{-1}	μM^{-1}
α(Fe)	Ni, Mg hybrids (this work)	pH 6.5, 7.4, 25 °C	−	0.16 ± 0.03	ND	ND
			+	0.12 ± 0.01	0.21	0.57
	Mn(II) hybrids (20)	pH 6.6, 25 °C	−	0.15	0.11	1.3
			+	0.11	0.14	0.78
	Fe(III)CN/Fe(II) hybrids (17)	pH 6.6, 20 °C	+	0.18	ND	ND
	Co(II)/Fe(II) (19)	pH 7.0, 20 °C	−	0.11	ND	ND
			+	0.06	ND	ND
	Mutant hybrids (50)	pH 7.0, 20 °C	−	0.12 ± 0.03	ND	ND
			+	0.10 ± 0.04	ND	ND
	Native HbA_0 (14)	pH 7.4, 25 °C	−	0.10 ± 0.04	ND	ND
β(Fe)	Ni, Mg hybrids (this work)	pH 6.5, 7.4, 25 °C	−	0.07 ± 0.02	ND	ND
			+	0.05 ± 0.01	0.19	0.22
	Mn(II) hybrids (20)	pH 6.6, 25 °C	−	0.13	0.16	0.80
			+	0.05	0.19	0.26
	Fe(III)CN/Fe(II) hybrids (17)	pH 6.6, 20 °C	+	0.07	ND	ND
	Co(II)/Fe(II) hybrids (19)	pH 7.0, 20 °C	−	0.10	ND	ND
			+	0.04	ND	ND
	Mutant hybrids (50)	pH 7.0, 20 °C	−	0.18 ± 0.05	ND	ND
			+	0.14 ± 0.04	ND	ND
	Native HbA_0 (14)	pH 7.4, 25 °C	−	0.15 ± 0.02	ND	ND

TABLE VII

Rate and equilibrium constants for O_2 binding to the R or T states of hemoglobin A_0, O_2 binding to the R quaternary state

The k'_{RO2} values for this work were computed as the average of fast association rate constants for O_2 rebinding to the Fe(II)/Cr(III) and Fe(II)/Mn(III) hybrids at pH 6.5, 7.4, and 8.4 in the absence of IHP (Table III, part A). The k_{RO2} values were computed from the average of those observed for the Fe(II)/Cr(III) and Fe(II)/Mn(III) hybrids at pH 6.5, 7.4, and 8.4 (Table IV, part A). The equilibrium constants for O_2 binding to the subunits within R state hemoglobin were calculated from the ratio of the rate constants, $K_{RO2} = k'_{RO2}/k_{RO2}$. The parameters based on the metal hybrids are compared to those obtained from analyzing mutant hybrids (50) and native human hemoglobin using *p*-hydroxybenzoate modification of βCys93 to enhance the differences between the subunits (12).

Subunit	Hemoglobin (Ref.)	Condition	k'_{RO2}	k_{RO2}	K_{RO2}
			$\mu M^{-1}\ s^{-1}$	s^{-1}	μM^{-1}
α(Fe)	Cr(III), Mn(III) hybrids (this work)	pH 6.5 to 8.4, 25 °C	36 ± 3	16 ± 7	2.3 ± 1.2
	Mutant hybrids (50)	pH 7.0, 20 °C	28 ± 9	12 ± 3	2.3 ± 0.9
	Native HbA_0 (12)	pH 7.4, 25 °C	43 ± 8	12 ± 2	3.5 ± 1.0
β(Fe)	Cr(III), Mn(III) hybrids (this work)	pH 6.5 to 8.4, 25 °C	76 ± 8	32 ± 8	2.4 ± 0.9
	Mutant hybrids (50)	pH 7.0, 20 °C	100 ± 13	22 ± 8	4.5 ± 1.5
	Native HbA_0 (12)	pH 7.4, 25 °C	150 ± 30	40 ± 8	3.7 ± 1.1

more accurate estimate of the T state dissociation rate constants since the *y* intercepts are more poorly defined than either K_{O_2} or k'_{O_2}. This analysis suggests that the T state α(Fe) and β(Fe) subunits have roughly equal rate and equilibrium constants for O_2 binding in the absence of IHP at pH 7.4: $k'_{O_2} \approx 6\ \mu M^{-1}\ s^{-1}$; $k_{O_2} \approx 500\ s^{-1}$; and $K_{O_2} \approx 0.012\ \mu M^{-1}$ for both subunits.

Shibayama *et al.* (22) came to the same conclusions. Their assignments were based on kinetic data for Ni(II) hybrids measured in 0.1 M phosphate, pH 6.6, 20 °C. The α(Fe)- and β(Fe)-containing hybrids showed very similar association and dissociation rate constants with $k'_{O_2} \approx 6\ \mu M^{-1}$ and $k_{O_2} \approx 2000\ s^{-1}$. The higher dissociation rate constant is probably due to the presence of inorganic phosphate and the lower pH value.

TABLE VIII

Rate and equilibrium constants for O_2 binding to the R and T states of hemoglobin A_0, O_2 binding to the T quaternary state

The k'_{TO2} values for this work were computed as the average of slow association rate constants for O_2 binding to the Ni(II)- and Mg(II)/Fe(II) hybrids at pH 7.4 in the absence and presence of 100 μM of IHP (Table III, part B). The equilibrium constants for O_2 binding to the subunits within T state hemoglobin, K_{TO2}, were computed as the average of the first constant (K_1) determined in oxygen equilibrium curve measurements for Fe(II)/Ni(II) and Fe(II)/Mg(II) hybrids at pH 7.4 in the presence and absence of IHP (35, 36).[2] The k_{TO2} values were computed as k'_{TO2}/K_{TO2}. The values in parentheses for k_{TO2} are the average of the values listed in Table IV, part B which were obtained from the y intercepts in Fig. 7. The values in parentheses for K_{TO2} were computed from the rate constants in Tables III, part B and IV, part B. Our data at pH 7.4 is compared to that reported by Shibayama *et al.* (22) for O_2 binding to Fe(II)/Ni(II) hybrids at pH 6.6 in 0.1 M phosphate buffer.

Subunit	Hemoglobin (Ref.)	Condition	IHP	k'_{TO2}	k_{TO2}	K_{TO2}
				$\mu M^{-1}\ s^{-1}$	s^{-1}	μM^{-1}
α(Fe)	Ni, Mg hybrids (this work)	pH 7.4, 25 °C	−	5.6	430 (400)	0.013 (0.014)
			+	11	3,700 (4,800)	0.0030 (0.0023)
	Ni hybrids (22)	pH 6.6, 20 °C	−	4.8	2,000	0.0024
β(Fe)	Ni, Mg hybrids (this work)	pH 7.4, 25 °C	−	6.7	670 (650)	0.010 (0.010)
			+	4.9	1,800 (1,700)	0.0027 (0.027)
	Ni hybrids (22)	pH 6.6, 20 °C	−	7.5	2,000	0.0038

These workers and others (22, 35, 36)[2] have shown that the exact ligand binding parameters of the low affinity hybrids are strongly dependent on pH and organic phosphate binding implying more that one T state. In agreement with many previous studies, dramatic effects on the T state O_2 binding parameters are seen when IHP is added to the Ni(II) and Mg(II) hybrids at pH 7.4 (Table VIII). The overall oxygen affinities for both T state subunits decrease ~4-fold, but the α(Fe) subunits show 2-fold higher association and dissociation rate constants than the β(Fe) subunits. $k'_{\alpha O_2} = 11\ \mu M^{-1}\ s^{-1}$ *versus* $k'_{\beta O_2} = 5\ \mu M^{-1}\ s^{-1}$ and $k_{\alpha O_2} \approx 3700\ s^{-1}$ *versus* $k_{\beta O_2} \approx 1800\ s^{-1}$ in the presence of IHP. This situation is the exact opposite of what occurs in the R state, where the β(Fe) subunits equilibrate more rapidly with O_2 than the α(Fe) subunits.

Importance of Equal O_2 Affinities of the α and β Subunits—The results in Tables VII and VIII show unequivocally that the equilibrium constants for O_2 binding to the individual subunits are very similar to each other in the low affinity and high affinity hybrids, both in the absence and presence of inositol hexaphosphate. Thus, Perutz's original mechanism that proposed an ordered addition of ligands is not correct. The equilibrium functional equivalence is still surprising since the structural mechanisms that cause the 500–1000-fold decrease in affinity in going from the R to T state are still thought to be quite different for the two subunits. Based on recent site-directed mutagenesis studies, steric hindrance by distal residues does appear to play a key role in regulating oxygen affinity in β subunits, whereas proximal constraints on iron reactivity are thought to be more important in α subunits (1, 49, 60–63).

The absence of chain differences does enhance the physiological activity of Hb by maximizing the Hill coefficient or n value for the native tetramer. The extent of O_2 transport is directly related to the slope of the oxygen equilibrium curve as follows: the higher the n value, the greater the amount of O_2 transported per iron atom. Large intrinsic differences between the O_2 affinities of the α and β subunits in both the high and low affinity quaternary states would decrease the extent of cooperativity, causing a marked reduction in transport. Instead, the subunits in Hb A_0 have evolved to have similar affinities giving rise to high n values and efficient O_2 transport.

REFERENCES

1. Perutz, M. F. (1970) *Nature* **228,** 726–739
2. Maxwell, J. C., and Caughey, W. S. (1976) *Biochemistry* **15,** 388–396
3. Olson, J. S. (1981) *Methods Enzymol.* **76,** 631–651
4. Perutz, M. F., Fermi, G., Luisi, B., Shaanan, B., and Liddington, R. C. (1987) *Acc. Chem. Res.* **20,** 309–321
5. Paoli, M., Dodson, G., Liddington, R. C., Wilkinson, A. J. (1997) *J. Mol. Biol.* **271,** 161–167
6. Gibson, Q. H., Parkhurst, L. J., and Geraci, G. (1969) *J. Biol. Chem.* **244,** 4668–4676
7. Olson, J. S., and Gibson, Q. H. (1971) *J. Biol. Chem.* **246,** 5241–5253
8. Olson, J. S., Andersen, M. E., and Gibson, Q. H. (1971) *J. Biol. Chem.* **246,** 5919–5923
9. Olson, J. S., and Gibson, Q. H. (1972) *J. Biol. Chem.* **247,** 1713–1726
10. Gibson, Q. H. (1973) *Proc. Natl. Acad. Sci. U. S. A.* **70,** 1–4
11. Ho, C. (1992) *Adv. Protein Chem.* **43,** 153–312
12. Vandegriff, K. D., Le Tellier, Y. C., Winslow, R. M., Rohlfs, R. J., and Olson, J. S. (1991) *J. Biol. Chem.* **266,** 17049–17059
13. Mathews A. J., and Olson, J. S. (1994) *Methods Enzymol.* **232,** 363–386
14. Perrella, M., Davids, N., and Rossi-Bernardi, L. (1992) *J. Biol. Chem.* **267,** 8744–8751
15. Liddington, R., Derewenda, Z., Dodson, E., Hubbard, R., and Dodson, G. (1992) *J. Mol. Biol.* **228,** 551–579
16. Brunori, M., Amiconi, G, Antonini, E, and Wyman, J. (1970) *J. Mol. Biol.* **49,** 461–471
17. Cassoly, R., and Gibson, Q. H. (1972) *J. Biol. Chem.* **247,** 7332–7341
18. Hoffman, B. M., Gibson, Q. H., Bull, C., Crepeau, R. H., Edelstein, S. J., Fisher, R. G., and McDonald, M. J. (1975) *Ann. N. Y. Acad. Sci.* **244,** 174–186
19. Ikeda-Saito, M., and Yonetani, T. (1980) *J. Mol. Chem.* **138,** 845–858
20. Blough, N. V., and Hoffman, B. M. (1982) *J. Am. Chem. Soc.* **104,** 4247–4250
21. Blough, N. V., and Hoffman, B. M. (1984) *Biochemistry* **23,** 2875–2882
22. Shibayama, N., Yonetani, T., Regan, R. M., and Gibson, Q. H. (1995) *Biochemistry* **34,** 14658–14667
23. Philo, J. S., Dreyer, U., and Lary, J. W. (1996) *Biophys. J.* **70,** 1949–1965
24. Unzai, S., Hori, H., Miyazaki, G., Shibayama, N., and Morimoto, H. (1996) *J. Biol. Chem.* **271,** 12451–12456
25. Imai, K. (1973) *Biochemistry* **12,** 798–808
26. Imai, K. (1982) *Allosteric Effects in Haemoglobin*, pp. 218–229, Cambridge University Press, Cambridge
27. Silva, M. M., Rogers, P. H., and Arnone, A. (1992) *J. Biol. Chem.* **267,** 17248–17256
28. Paoli, M., Liddington, R., Tame, J., Wilkinson, A., and Dodson, G. (1996) *J. Mol. Biol.* **256,** 775–792
29. Schumacher, M. A., Zheleznova, E. E., Poundstone, K. S., Kluger, R., Jones, R. T., Brennan, R. G. (1997) *Proc. Natl. Acad. Sci. U. S. A.* **94,** 7841–4844
30. Daugherty, M. A., Shea, M. A., Johnson, J. A., LiCata, V. J., Turner, G. J., and Ackers, G. K. (1991) *Proc. Natl. Acad. Sci. U. S. A.* **88,** 1110–1114
31. Ackers, G. K., Doyle, M. L., Myers, D., and Daugherty, M. A. (1992) *Science* **255,** 54–63
32. Ackers, G. K., Perrella, M., Holt, J. M., Denisov, I., and Huang, Y. (1997) *Biochemistry* **36,** 10822–10829
33. Shibayama, N., Morimoto, H., and Saigo, S. (1997) *Biochemistry* **36,** 4375–4381
34. Shibayama, N., Morimoto, H., and Saigo, S. (1998) *Biochemistry* **37,** 6221–6228
35. Shibayama, N., Morimoto, H., and Miyazaki, G. (1986) *J. Mol. Biol.* **192,** 323–329
36. Shibayama, N., Morimoto, H., and Kitagawa, T. (1986) *J. Mol. Biol.* **192,** 331–336
37. Luisi, B., and Shibayama, N. (1989) *J. Mol. Biol.* **206,** 723–736
38. Luisi, B., Liddington, B., Fermi, G., and Shibayama, N., (1990) *J. Mol. Biol.* **214,** 7–14
39. Park, S. Y., Nakagawa, A., and Morimoto, H. (1996) *J. Mol. Chem.* **255,** 726–734
40. Earley, J. E., and Cannon, R. D. (1965) *Transition Metal Chem.* **1,** 33–109
41. Buchler, J. W. (1975) in *Porphyrins and Metalloporphyrins* (Smith, K. M., ed) pp.191–195, Elsevier Science Publishers B.V., Amsterdam
42. Summerville, D. A., Jones, R. D., Hoffman, B. M., and Basolo, F. (1977) *J. Am. Chem. Soc.* **99,** 25, 8195–8202
43. Balch, A. L., Latos-Grazynski, L., Noll, B. C., Olmstead, M. M., and Zovinka, E. P. (1992) *Inorg. Chem.* **31,** 1148–1151
44. Shibayama, N., Imai, K., Morimoto, H., and Saigo, S. (1995) *Biochemistry* **34,** 4773–4780
45. Olson, J. S., Eich, R. F., Smith, L. P., Warren, J. J., and Knowles, B. C. (1997) *BioTechnology* **25,** 227–241
46. Kroeger, K. S., and Kundrot, C. E. (1997) *Structure* **5,** 227–237
47. Fujii, M., Hori, H., Miyazaki, G., Morimoto, H., and Yonetani, T. (1993) *J. Biol. Chem.* **268,** 15386–15393
48. Waterman, M. R., and Yonetani, T. (1970) *J. Biol. Chem.* **245,** 5847–5852
49. Mathews, A. J., Olson, J. S., Renaud, J.-P., Tame, J., and Nagai, K. (1991)

J. Biol. Chem. **266,** 21631–21639
50. Mathews, A. J., Rohlfs, R. J., Olson, J. S., Tame, J., Renaud, J.-P., and Nagai, K. (1989) *J. Biol. Chem.* **264,** 16573–16583
51. Rohlfs, R. J., Mathews, A. J., Carver, T. E., Olson, J. S., Springer, B. A., Egeberg, K. D., and Sliger, S. G. (1990) *J. Biol. Chem.* **265,** 3168–3176
52. Philo, J. S., and Lary, J. W. (1990) *J. Biol. Chem.* **265,** 139–143
53. Sharma, V. S., Schmidt, M. R., and Ranney, H. M. (1976) *J. Biol. Chem.* **251,** 4267–4272
54. Sharma, V. S., Bandyopadhyay, D., Berjis, M., Rifkind, J., and Boss, G. R. (1991) *J. Biol. Chem.* **266,** 24492–24497
55. Simolo, K., Stucky, G., Chen, S., Bailey, M., Scholes, C., and McLendon, G. (1985) *J. Am. Chem. Soc.* **107,** 2865–2872
56. Samaja, M., Rovida, E., Niggeler, M., Perrella, M., and Rossi-Bernardi, L. (1987) *J. Biol. Chem.* **262,** 4528–4533
57. Kuila, D. K., Natan, M. J., Rogers, P., Gingrich, D. J., Baxter, W. W., Arnone, A., and Hoffman, B. M. (1991) *J. Am. Chem. Soc.* **113,** 6520–6526
58. Fronticelli, C., Brinigar, W. S., Olson, J. S., Bucci, E., Gryczynski, Z., O'Donnel, J. K., and Kowalczyk, J. (1993) *Biochemistry* **32,** 1235–1242
59. Sawicki, C. A., and Gibson, Q. H. (1977) *J. Biol. Chem.* **252,** 7538–7547
60. Hille, C. R., Olson, J. S., and Palmer, G. A. (1979) *J. Biol. Chem.* **254,** 12110–12120
61. Nagai, K., Luisi, G., Shih, D., Miyazaki, G., Imai, K., Poyart, C., DeYoung, A., Kwiatkowsky, L., Noble, R. W., Lin S.-H., and Yu, N. T. (1987) *Nature* **329,** 858–860
62. Perutz, M. F. (1989) *Trends Biochem. Sci.* **14,** 42–44
63. Tame, J., Shih, D. T.-B., Pagnier J., Fermi,, G., and Nagai, K. (1991) *J. Mol. Biol.* **218,** 761–767